Electronic Supplementary Material (ESI) for Journal of Materials Chemistry C.
This journal is © The Royal Society of Chemistry 2021

Supporting Information

Stabilizing $TiO_2/CH_3NH_3PbI_3$ Heterostructure and Enhancing Interface Trap Passivation for Efficient and Stable Perovskite Solar Cells

Shendong Xu,[ab] Zheng Liang,[ab] Haiying Zheng,[d] Liying Zhang,[ab] Xiaoxiao Xu,[ab] Huifen Xu,[ad] Liangzheng Zhu,[c] Jiajiu Ye,[a] Guozhen Liu,[a]* Xu Pan[a]*

[a]Key Laboratory of Photovoltaic and Energy Conservation Materials, Institute of Solid State Physics, Hefei Institutes of Physical Science, Chinese Academy of Sciences, Hefei 230031, China.

[b]University of Science and Technology of China, Hefei 230026, China.

[c]Anhui Province Key Laboratory of Condensed Matter Physics at Extreme Conditions, High Magnetic Field Laboratory, Chinese Academy of Science, Hefei 230031, Anhui, China.

[d]Institutes of Physical Science and Information Technology, Anhui University, Hefei, 230601, China.

Keywords: perovskite solar cells, interfacial modification, soft perovskite heterostructure, efficiency and stability

Experimental section

Materials

The tetrabutylammonium borohydride (TABH) were purchased from aladdin.

Titanium(diisopropoxide) bis(2,4-pentanedionate) is supplied by Alfa. The TiO_2 paste from Greatcell solar. Methylammonium iodide (MAI) and Spiro-MeOTAD both purchased from Xi'an Polymer Light Technology manufacturers. The lead(II) iodide (PbI_2) were purchased from TCI. DMSO (dimethylsulfoxide 99.50%) and DMF (N,N-dimethylformamide 99.99%) from Sinopharm. Other materials have been acquired from Sinopharm or Alfa or Aldrich and all the commercial materials were used as received without additional treatment.

Perovskite Solar Cells (PSCs) Fabrication

The device was fabricated by the one-step method according to previous reports. Device structure is FTO/compact-TiO_2/ mesoporous-TiO_2/perovskite/ spiro-MeOTAD/Au. Firstly, a compact TiO_2 layer was coated on the FTO by spray pyrolysis using high purity nitrogen as carrying gas at 450 °C hold for 40 minutes and the Titanium(diisopropoxide) bis(2,4-pentanedionate) precursor was diluted 10 times with isopropanol solution. Then, we diluted the titanium dioxide paste (30 nm) with anhydrous ethanol in a ratio of 1:5.5(Weight ratio). Then, the diluted paste spin coating on the compact TiO_2 layer basement, after the spin coating, put film in a titanium plate furnace for sintering, the sintering temperature from room temperature slowly rising to 510 °C, keep 3 hours, finally the formation of mesoporous TiO_2 layer. Then, TABH isopropanol solution was spin-coated on mesoporous TiO_2 layer and annealed at 100 ℃ for 10 minutes. The Pb^{2+} precursor solutions of $MAPbI_3$ was fabricated by dissolving the corresponding amount of MAI and PbI_2 powders in anhydrous N,N-dimethylformamide (DMF) and dimethyl sulfoxide (DMSO) mixed

solvent (DMF:DMSO = 1:4) with stirring at 50 °C for 30 min. The perovskite layers were coated by spin coating 1.4M Pb^{2+} perovskite precursor solutions in dry air(humidity was kept at about 10% RH) flowing glovebox. Chlorobenzene (100 μL) was dropwise added on the substrate during the spin-coating step 15s before the end of the total procedures. The substrate was sintered at 105 °C for 50 min on a hotplate. After cooling to room temperature, the hole-transporting material (HTM) solution was deposited on the perovskite layer by spin coating which was comprised of spiro-OMeTAD(73.5mg), 4-tert-butylpyridine, cobalt(III) salt and lithium bis-(trifluoromethanesulfonyl)imide and in chlorobenzene solvent. Finally, the films were dried under vacuum before completing the device fabrication process by thermal evaporating 60 nm of Au on top of the HTM layer.

Characterization

PCEs and *J-V* curves were obtained via using a solar simulator (Newport, Oriel Class A, 91195A) and a source meter (Keithley 2420). SEM images were performed on a field-emission scanning electron microscope (FE-SEM, sirion200, FEI Corp., Holland) with high-resolution. The Ultraviolet–visible absorption spectra were obtained from ultraviolet-vis (UV-vis) spectrophotometer(U-3900H, HITACHI, Japan). Steady-state PL spectra were obtained from a spectrofluorometer (photon technology international). The exciting wavelength was 473 nm and excited by a standard 450 W xenon CW lamp and analyzed by the software Fluorescence. The time-resolved PL experiments were performed with the same Fluorescence Lifetime Spectrofluorometer using a

pulsed source at 450 nm (the illumination source is a pulsed nitrogen dye laser) and the signal was recorded at 770 nm by the Time Correlated Single Photon Counting (TCSPC) technique. XPS data was obtained from Thermo ESCALAB 250Xi system. EIS at -0.6 V was tested on an Autolab analyzer(Metrohm, PGSTAT 302N, Switzerland) in the dark with a frequency range from 0.1 Hz to 1 MHz. IPCE with a wavelength range from 300 to 900 nm were tested with dual Xenon/quartz halogen light source (PV Measurements, Inc.), and measured in DC mode with no bias light used. The solar simulator with 100 mW/cm^2 illumination AM 1.5G was calibrated via a Si-reference cell which was certified by NREL. Via masking a black mask, the devices retained an active area of 0.09 cm^2.

Devices Aging Test

Ultraviolet aging is to place the device directly under the ultraviolet lamp and continuously receive ultraviolet light irradiation. Humidity aging involves placing the device in an opaque vessel in contact with the atmosphere(40% to 60% RH). The opaque vessel was kept at room temperature (about 25 °C). Heat aging test was performed at 85 °C in a vacuum oven. The vacuum oven with about 5% RH was placed in the dark.

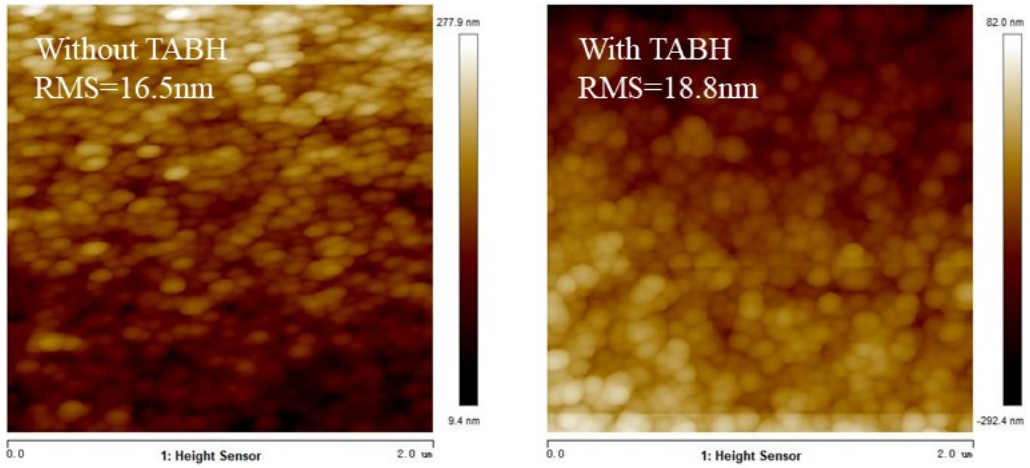

Fig. S1. AFM height images (2 μm × 2 μm) of perovskite films with TABH and without TABH. RMS: root-mean-square.

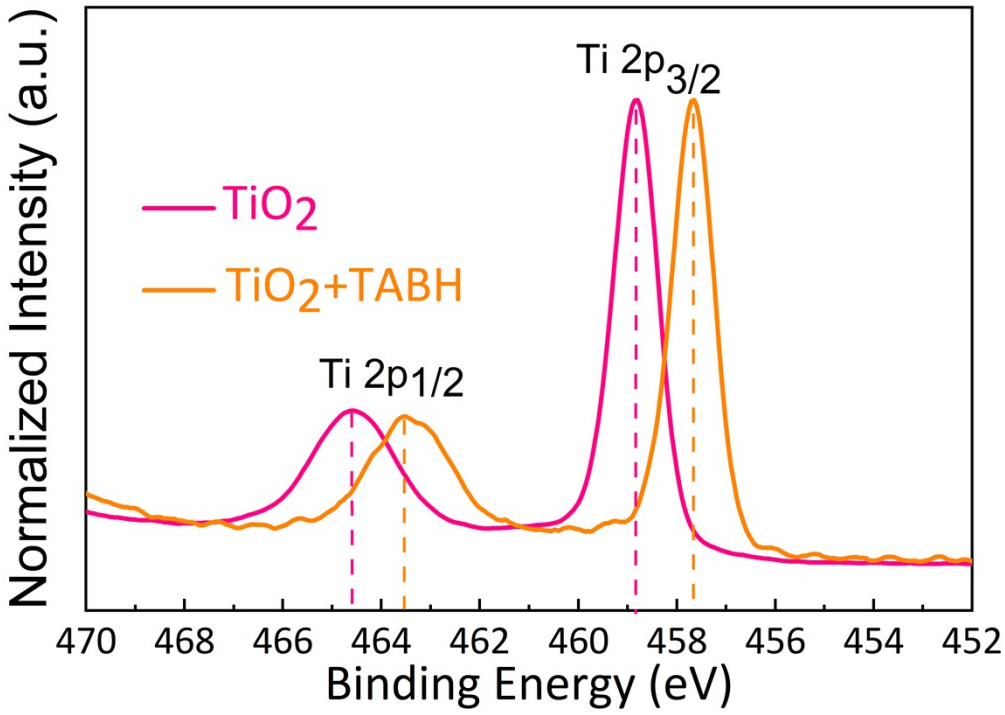

Fig. S2. High-resolution XPS Ti2p spectra with and without TABH.

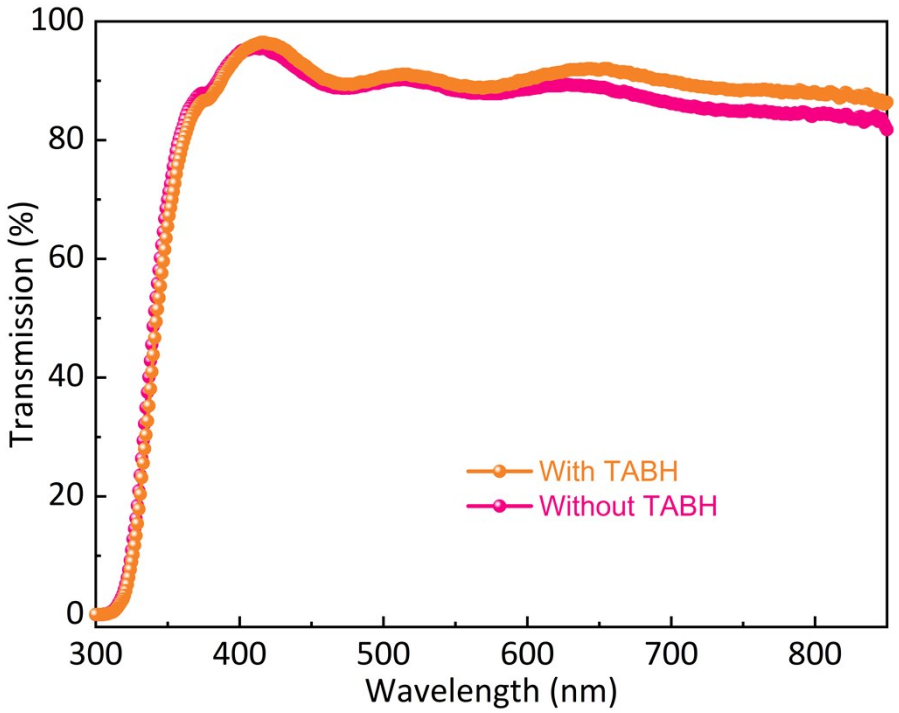

Fig. S3. Transmission spectra of the unmodified TiO_2 and the TABH modified TiO2 films.

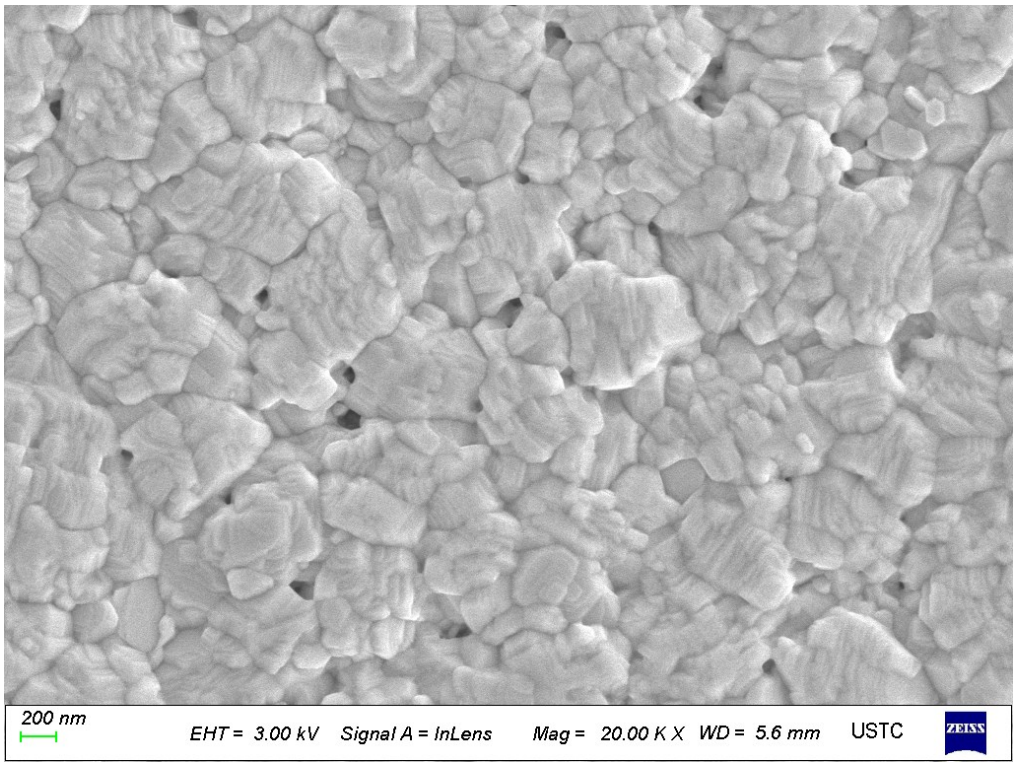

Fig. S4. Top-view SEM images of perovskite films without TABH.

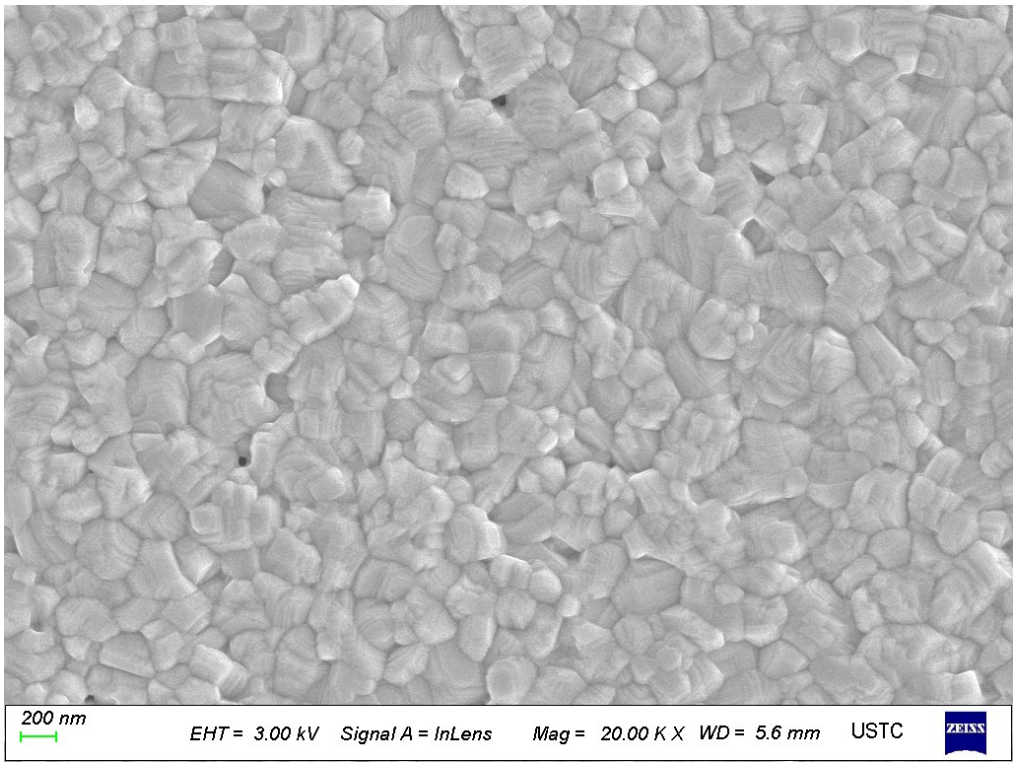

Fig. S5. Top-view SEM images of perovskite films with TABH.

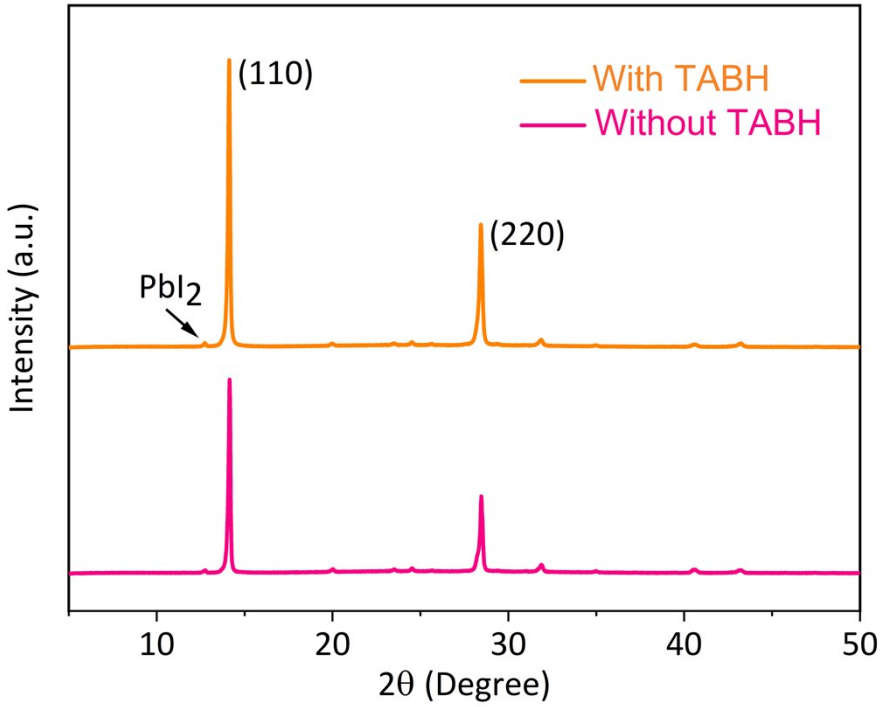

Fig. S6. XRD patterns of perovskite thin films with and without TABH.

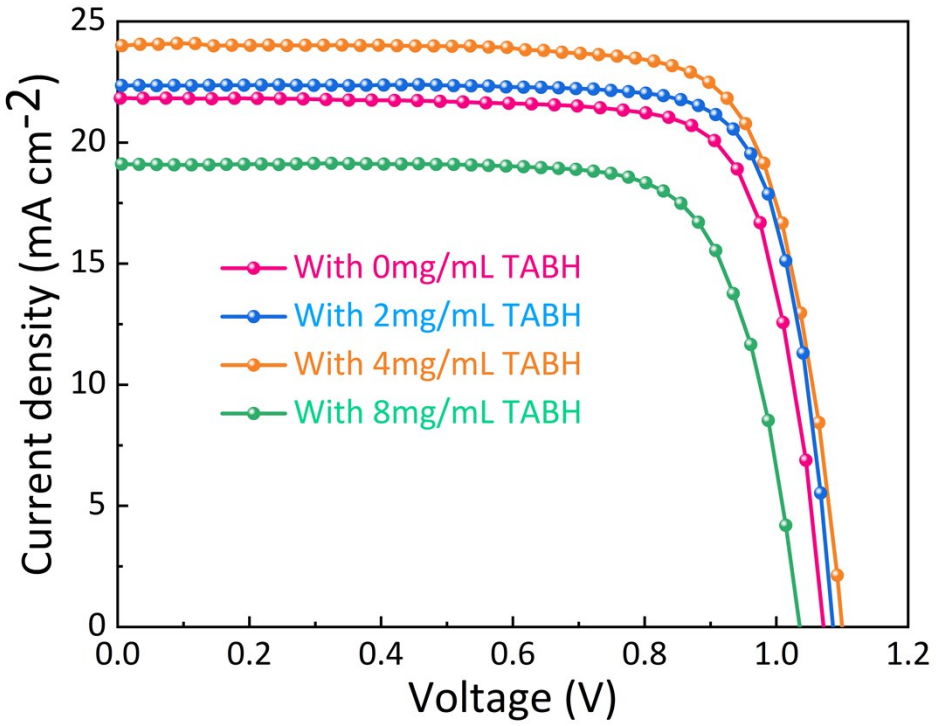

Fig. S7. *J*−*V* curves of PSCs with different concentrations of TABH modified.

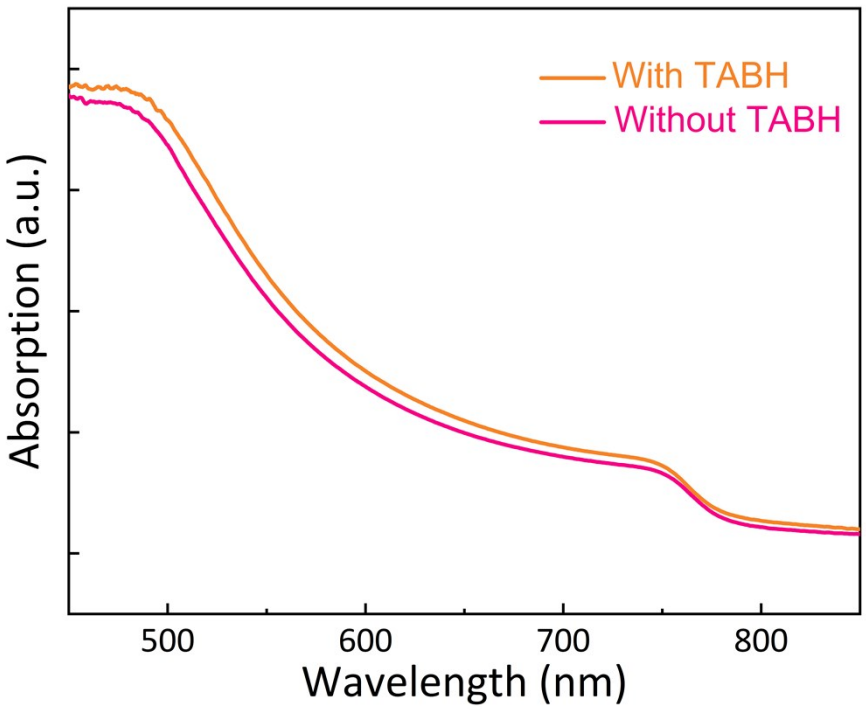

Fig. S8. Ultraviolet−visible absorption spectra.

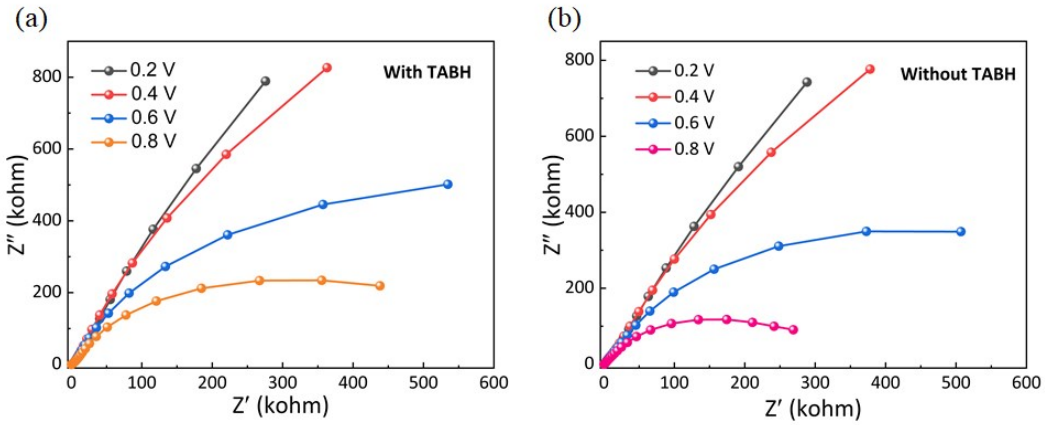

Fig. S9. Nyquist plots of control and TABH modified devices recorded at different bias voltages.

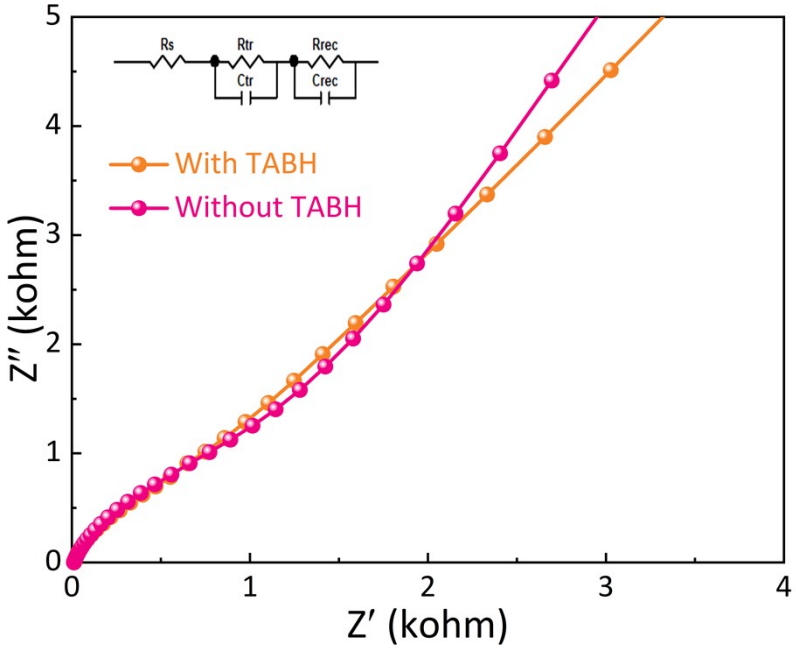

Fig. S10. Nyquist plots of PSCs with and without TABH obtained at a bias of 0.8 V in high frequency range.

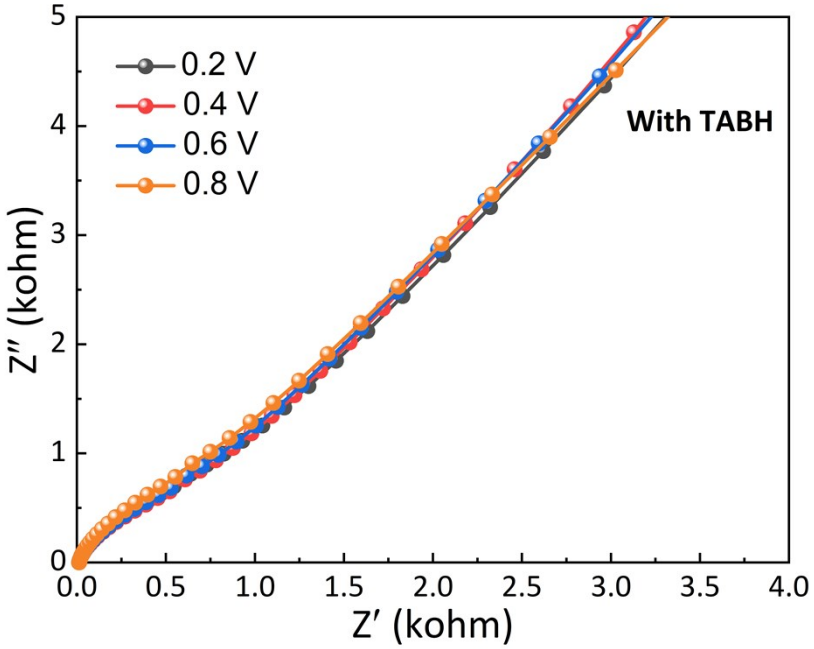

Fig. S11. Nyquist plots of TABH modified devices recorded at different bias voltages in high frequency range.

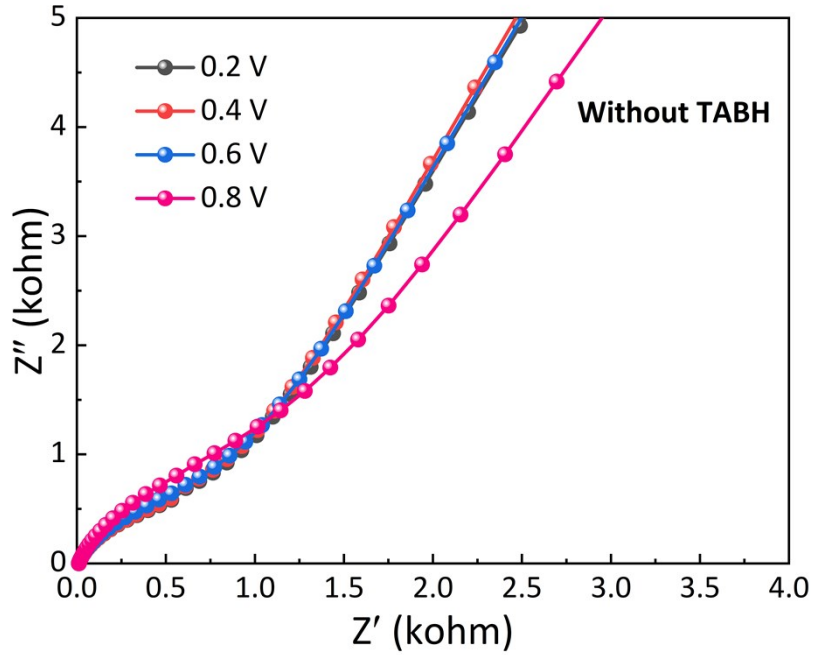

Fig. S12. Nyquist plots of control devices recorded at different bias voltages in high frequency range.

Table S1. Fitted results of TRPL curves in Figure 4b using a single-exponential decay

equation of $I(t)=I_0+A_1\exp(-t/\tau)$, where τ represent slow decay time constant.

Devices	I_0	A_1	τ (ns)
Without TABH	149.66	221.85	31.56
With TABH	55.46	327.71	24.00

Table S2. Fitted results of EIS with TABH.

Bias voltages (V)	High frequency resistance(Ω)	Low frequency resistance(Ω)
0.2	2123	$1.09*10^6$
0.4	1888	$1.16*10^6$
0.6	1938	$6.80*10^5$
0.8	2258	$3.89*10^5$

Table S3. Fitted results of EIS without TABH.

Bias voltages (V)	High frequency resistance(Ω)	Low frequency resistance(Ω)
0.2	1204	$9.40*10^5$
0.4	1211	$9.73*10^5$
0.6	1228	$5.21*10^5$
0.8	1745	$2.20*10^5$